Technical Reference for

The CLEVER Model

– A Real-time Flood Forecasting Model for British Columbia

By

Dr. Charles Luo, P.Eng.

Forecasting Hydrologist

BC River Forecast Centre

3rd Floor, 395 Waterfront Crescent, Victoria, BC V8T 5K7, Canada.

E-mail address: Charles.Luo@gov.bc.ca

First prepared on November 9, 2015

Latest updated on August 16, 2017

This page is blank.

Table of Contents

List of figures

List of Tables

Abstract

The watersheds in British Columbia (BC) are characterized by their huge scale. A real-time flood forecast model for the watersheds in BC should be able to tackle the issues related to the huge scale and still be time efficient. The Channel Links Evolution Efficient Routing Model is developed for this purpose. In the model, a huge-scale, heterogeneous watershed is divided into a number of smaller and relatively homogeneous subcatchments which are further simplified into individual nodes connected with channel links. This hybrid model consists of a lumped watershed routing sub-model and a distributed, physics-based open channel routing sub-model. The watershed routing sub-model routes the net water input to each subcatchment with the instantaneous unit hydrograph and provides input as boundary conditions to the channel routing sub-model, which routes the channel links with an innovated numerical scheme similar to the Semi-Implicit Method for Pressure-Linked equations (SIMPLE) to solve the kinematic wave equations. The outputs from the actual real-time model operation of flood forecasting in 2015 freshet season are evaluated extensively. The evaluation results demonstrate that the model is time efficient for real-time flood forecasting in the huge-scale watersheds in BC with reasonable accuracy.

Keywords: Large-scale watershed, real-time flood forecasting, hybrid model, Kinematic wave, temperature-index

1. Introduction

British Columbia (BC), the third largest province in Canada, has a huge area (947,900 km^2) which is the combined size of France, Italy, Belgium and the Netherlands (Wood, 2001). In the meantime, its geological and geomorphological variety is immense (Foster, 2001). The province is abundant with rivers, creeks and lakes, with varied terrain from steep mountains to coastal lowlands and equally varied weather and climate. The total number of rivers and creeks is about 24,000 (Smith, 2001) and the total length of rivers and creeks within BC is approximately 42,150 km. BC has the greatest amount of fresh water in Canada (McGillivray, 2005). However, accompanying this abundance of water resources are floods, which are the most damaging natural hazards in BC (Foster, 2001). Consequently, real-time flood forecasts and timely flood warnings are important in BC. Flood forecasting involves an operational flood forecasting system, which plays a key role in preparedness for possible flood disasters by providing early warnings up to several days ahead of the flood events to the related authorities and the public (Penning-Rowsell et al., 2000; Patrick, 2002).

A numerical computer model is the core element of a flood forecasting system. Over the past decades, many hydrological models have been developed and especially in the recent 15 years, flood

forecasting techniques have advanced considerably. Data-driven models, particularly the neural networks (NN) models, such as Chiang et al. (2007), Sahoo et al. (2006) and Chau et al. (2005), have been widely used in flow forecasting due to their simplicity (Hapuarachchi et al., 2011). The disadvantages of data-driven models for flood forecasting are their requirements of long-term data records and the site specificity of the derived relationships (Hapuarachchi et al., 2011). Besides the data-driven models, recently developed lumped models, such as Sirdas and Sen (2007) and Foody et al. (2004), are also used for flood forecasting. One of the limitations of using lumped models for flood forecasting is their coarse resolution (Hapuarachchi et al., 2011). On the other hand, a number of physics-based, distributed hydrological models have been developed, such as BTOP (Takeuchi et al., 2008), LUOM (Luo, 2007) and MARINE (Estupina-Borrell et al., 2006), in recent years. However, the physics-based, distributed models require intensive watershed data and their computing time is much longer than other types of models.

Selection of an appropriate hydrological model for real-time flood forecasting in BC's watersheds must be based on the watershed characteristics and the features of real-time flood forecasting. Lyons (1976) presented a computer program – SIMPAK, which was probably the first computer model that was applied to the Fraser River in BC for the purpose of flood forecasting by using the simple curvature-slope method applied to the observed hydrograph. Large errors were present in the forecasts by Lyons (1976), especially during the falling stage of the flow. However, the forecast results could be used as an indicator of the worst situation and would be greatly improved if weather and snow information were added to the model (Lyons, 1976). Quick and Pipes (1972) developed a water budget model for daily and seasonal runoff forecast in the Okanagan basin in BC. Based on this model, a relatively sophisticated model – the UBC Watershed model (Quick and Pipes, 1977) was developed, originally for daily streamflow forecasting in the Fraser River system in BC. In the model, meteorological data were used to simulate daily snowmelt in the watershed. However, the UBC Watershed Model was recommended to run for a complete annual hydrological cycle so as to permit important model aspects to be assessed (Quick and Pipes, 1977). Meanwhile, the UBC Watershed Model itself does not include a channel routing component and if it is required, a very simple lag-and-route model relying on the wave travel time (Quick and Pipes, 1975) is recommended. To forecast accurately the peak and peaking time at the downstream locations of the huge-scale watersheds in BC, a more sophisticated physics-based channel routing model is necessary. Some of the fully distributed, physics-based watershed models also include a distributed, physics-based channel routing model, and therefore are given the first try for real-time flood forecasting in this study.

The watersheds in BC are characterized by their huge scale which a real-time flood forecast model applied to BC's watersheds must first tackle. Large-scale watersheds always exhibit great heterogeneity and variability not only spatially but also temporally (Luo, 2000). The heterogeneity of a watershed is mainly from four sources: climate, topography, geology and land uses (Singh, 2012). Large

water bodies are also present in BC's watersheds, e.g., Stuart Lake in the Upper Fraser River watershed, which is about 66 km long and 10 km wide (maximum) and has a water surface area of 358 km^2. In order to easily simulate these large waterbodies, the Large-scale, Unified, and Optimization Model (LUOM), which is a fully distributed, physics-based watershed model for streamflow simulation in watersheds with large water bodies and channel loops (Luo, 2007; Luo, 2000), was selected for the first try for real-time flood forecasting. The maximum spatial step for the LUOM (Luo, 2007) is 1 km. Using this spatial step (1 km), the Fraser River basin (A=232,200 km^2) has a total of 232,200 grid cells. The LUOM (Luo, 2007) was subsequently established for the Fraser River basin with a spatial step of 1 km and a temporal step of 1 hour. The model consumed about 8 hours of computing time for a run of a 30-day period on a computer of 2.6 GHz CPU clock. This is obviously impractical for real-time flood forecasting in BC's watersheds.

This first try of using a fully distributed watershed model highlights the second issue that a real-time flood forecast model for BC's watersheds has to tackle. This is the model efficiency which enables the model to provide timely warnings to the related authorities and the public. In simple words, the model must be able to complete a run in a very short time, e.g., several minutes. This is critical because it is always the case that several calibrations of the model parameters are necessary each day due to the temporal variation of the representativeness of the observed climate data and that frequent updates of the forecasts are required due to rapidly changing conditions.

Based on the above analysis, a watershed model that compromises part of the model capability in addressing the issues related to the huge scale of the BC's watersheds for the sake of time efficiency in real-time flood forecasting is preferable to a totally lumped model or a fully distributed model, and a hybrid model is one solution. A hybrid model is a semi-distributed watershed model, in which distributed and lumped models are linked to each other (Aral and Gunduz, 2006). Aral and Gunduz (2006) presented a hybrid watershed modeling system, in which physics-based, distributed models for open channel flows and saturated groundwater flows are integrated with semi-empirical quasi-lumped-parameter models for overland flows and unsaturated flows. In this study, a different hybrid watershed model, the Channel Links Evolution Efficient Routing (CLEVER) Model, is developed for the purpose of real-time flood forecasting for the large-scale watersheds in BC. In the model, in order to tackle the heterogeneity, a large-scale watershed is split into a number of relatively homogeneous subcatchments which are further simplified into individual nodes, for which a lumped and conceptual watershed routing sub-model is developed. The subcatchments are connected with channel links, for which a one-dimensional, distributed open channel routing sub-model is developed. The two sub-models are integrated and the watershed routing sub-model provides inputs as boundary conditions to the open channel routing sub-model.

In the coming sections, the characteristics of the watersheds in BC are described briefly, and after that, the model development and evaluation are discussed in detail.

2. Study region - British Columbia and input data

Situated on the Pacific coast of Canada between latitudes 49° and 60° north, British Columbia is part of the North American Cordillera, the mighty set of mountain ranges that stretch from northern Alaska to southern Mexico, and 200 million years of geological activities resulted in the diverse landscape of British Columbia (Cannings, et al., 2011). The northeastern BC close to the border with Alberta is part of the Alberta Plateau which is geologically called the Interior Plains consisting of undeformed sediment. To the west of the Interior Plains is the so-called Foreland Belt, which is a narrow north-south region where the Rocky Mountains have been built. To the west of the Foreland Belt is the Omineca Belt, which is the slim north-south terrain of mountains and highlands consisting of intensely deformed and metamorphosed rock. The west coast mountains comprise the Coast Belt which is dominated by rock that was melted and recrystallized into immense granitic masses during the collision of plates. Between the Omineca Belt and the Coast Belt is the Intermontane Belt which is made up of plateaus, valleys and mountains. And the most western region of BC is the so-called Insular Belt which consists of the island mountains (Cannings, et al., 2011). As a consequence of these geomorphological distributions, approximately two-thirds of British Columbia are mountain slopes, rocky lands and water bodies (Dalichow, 1972). The elevation of BC ranges from 0 m (sea level) to 4671 m, which is the summit altitude of Fairweather Mountain located on the northwestern border with Alaska, USA (Wikipedia, 2015).

BC's soils have been largely formed by glacial drift (Dalichow, 1972) and may be classified into two types: forest-related soils on the coast and the grassland soils in the central interior (McGillivray, 2005). The topsoil of the two types is decomposing leaves or grasses. Below the topsoil of the forest-related soils to the bedrock are layers of grey soil, yellow to red hard pan, reddish brown loam, and hard parent material. Between the top soils of the grassland soils to the bedrock are, from top to bottom, layers of black soil, brown calcium carbonate, and greyish weathered bedrock (McGillivray, 2005).

Out of the total area of approximately 95 million hectares of British Columbia, almost 60% (55 million hectares) is covered by forests (plus an additional 3.7 million hectares with stunted or scattered trees), of which 83% is dominated by conifers. The five most common forest types are lodgepole pine, spruces, true firs, hemlocks, and Douglas-fir (B.C. Ministry of Forests, Mines and Lands, 2010).

British Columbia has three climate regions, Pacific, Cordilleran and Boreal (Hare and Thomas, 1974). The Pacific climate region includes coastal BC, which is influenced greatly by the Pacific Ocean and prevailing westerly winds and consequently is mild and wet in the winter and warm and dry in the summer. The Cordilleran climate region is defined by the mountain chains between the coastal

mountains and the Rocky Mountains (McGillivray, 2005) and the Boreal climate region is the northeastern plain. These two regions are affected by the frigid polar air during the winter season and thus most of the winter precipitation is in the form of snow. From south to north, winter temperatures in these regions decrease dramatically, e.g., from -3° to -23° Celsius in January. The most prominent feature of annual precipitation in BC is that its spatial distribution is highly affected by the north-south trending mountains with the larger amount of precipitation on the windward sides (Tuller, 2001). This means that the western sides of the coastal mountains have much larger annual precipitation than the eastern sides. Another feature is that northern BC, which is affected by the dry Arctic air, is drier than the southern parts of the province. The annual normal precipitation from 1981 to 2010 recorded at the following four climate stations gives a good example of these features (Environment Canada, 2015): 3184.4 mm at Estevan Point (Vancouver Island, western side of the coastal mountains), 349 mm at Lillooet Seton BCHPA (eastern side of the coastal mountains), 662.4 mm at Creston (southern BC), and 452.1 at Fort Nelson A (northern BC).

British Columbia has seven major watersheds, the Fraser River, the Columbia River (an international river), the Skeena River, the Nass River, the Stikine River, the Liard River (an interprovincial river), and the Peace River (an interprovincial river) (Fig. 1). From Fig. 1, it can be seen that the total drainage area of these seven watersheds excluding those parts outside BC is 726,986 km^2 (77% of the province land area) and the total length of rivers and their tributaries inside BC is 42,150 km. These and the other hydrometric characteristics are listed in Table 1.

Table 1. Major watersheds of British Columbia

Watershed	Total area within BC (km^2)	Total river length [a] (m)	Active WSC gauge station and (ID) [b]	% of area	Mean annual disch. (m^3/s)	Max disch. (m^3/s)	Year of max disch.	Years of records
Fraser	232136	11200	Fraser River at Hope (08MF005)	93	2717	15200	1948	102
Liard	142397	7000	Liard River at Lower Crossing (10BE001)	73	1163	9000	2012	74
Peace	123671	5300	Peace River near Taylor (07FD002)	82	1454	11500	1948	70
Columbia	103134	4900	Columbia River at Birchbank (08NE049)	85	2019	10600	1961	78
Skeena	54432	2700	Skeena River at Usk (08EF001)	78	914	9340	1948	87
Stikine	49648	2200	Stikine River at Telegraph Creek (08CE001)	58	429	3860	2007	60
Nass	21568	950	Nass River above Shumal Creek (08DB001)	85	814	9460	1961	85
Subtotal	726986	34250						
The rest of BC	220914	7900						
Total of BC	947900	42150						

[a] Total river length includes the length of the river and tributaries.
[b] WSC: Water Survey of Canada. The station is the available most downstream active WSC station with consecutive discharge records.

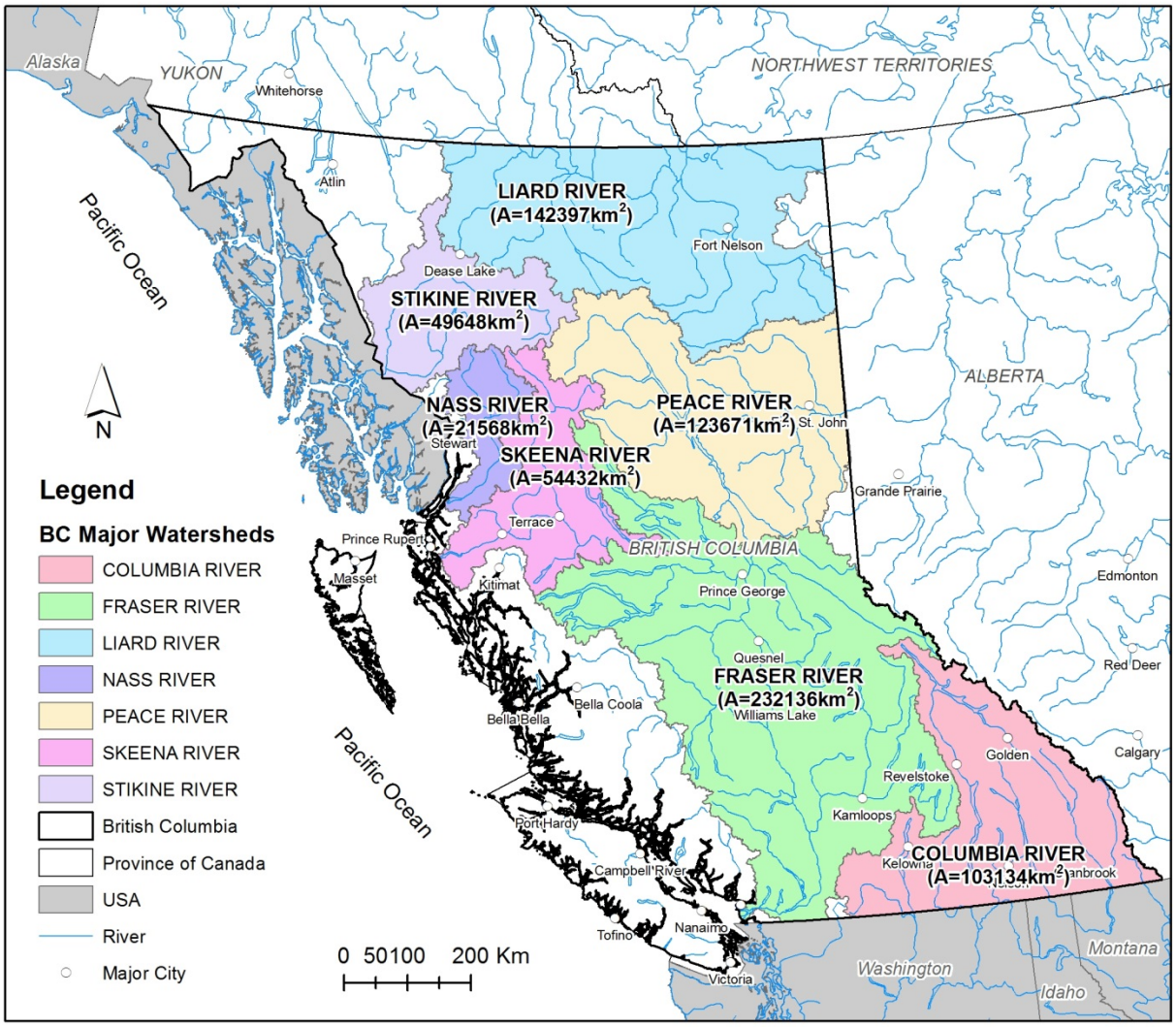

Figure 1. Seven major watersheds in British Columbia.

Across BC's watersheds there are a total of more than 300 Water Survey of Canada (WSC) real-time hydrometric stations which record real-time water levels and/or discharges of the rivers and creeks, approximately 250 Environment Canada (EC) climate stations, approximately 220 fire weather stations and 50 automated snow pillows (ASP) which record precipitation, temperature and other climate data. It is noticed that many short term flood forecasting systems rely on observed precipitation inputs which come initially from observation networks and radar (Cloke and Pappenberger, 2009). And for the snow-dominated watersheds in BC, daily precipitation, maximum and minimum temperatures provided by EC's climate stations and other climate stations are sufficient to drive short term flood forecast models. However, for medium (2–15 days ahead) and longer term forecasts, outputs from numerical weather prediction (NWP) models must be used (Hopson and Webster, 2010; Cloke and Pappenberger, 2009). The Meteorological Service of Canada provides 10-day forecast climate data from the Canadian

Meteorological Centre (CMC) NWP Models on local and global scales. In this study, Canadian Meteorological Centre's 10-day forecasts of precipitation and temperatures on both regional and global scales are downscaled to the locations of the available climate stations in BC. These hydrometric, climate and NWP data facilitate the real-time flood forecast modeling over the province by providing input and calibration data.

3. Methodology

3.1 Watershed simplification and model structure

HYMO (Williams and Hann, 1972, 1973) and the SWAT model (Arnold et al., 1998) divided a watershed into many small areas or subwatersheds according to their hydraulic characteristics and the hydrographs from these subwatersheds were the inputs of the stream flow routing. The HEC-1 (US Army Corps of Engineers, 1993) and HEC-HMS (US Army Corps of Engineers, 2000) models also have similar architecture. In this study, in order to address the watershed heterogeneity as much as possible, a large-scale watershed is first split into a number of relatively homogenous subcatchments which are further simplified into individual nodes that are located in the center of the subcatchments, rather than at the outlets of the subcatchments. A subcatchment is consequently treated as a single node and the water balance in the hydrologic cycle is calculated and then routed with the unit hydrograph. A channel link is created to connect the nodes of subcatchment and the outlet of the subcatchment, which is also the location of the flow gauge station that provides discharge data for model calibration. With this additional channel link connecting the node in the center of the subcatchment and the outlet of the subcatchment, the modeller has an addition tool or parameters to calibrate the timing of the hydrograph. If the flow gauge station is not located at the outlet of the entire watershed, more channel links are created to connect this station and its downstream stations until the flow reaches the watershed outlet. A channel link may have one or two inflows, one inflow if the channel link connects a subcatchment node and its outlet flow gauge station or there is only one upstream flow gauge station and no subcatchment node near around, or two inflows if the channel link has two upstream flow gauges stations nearby. The model capability that one channel link has two inflows or two upstream subcatchments makes the modeling more convenient when the outlets of two subcatchments are close to each other – this is always the case in BC's watersheds. Fig. 2 shows the process of watershed simplification and the model structure.

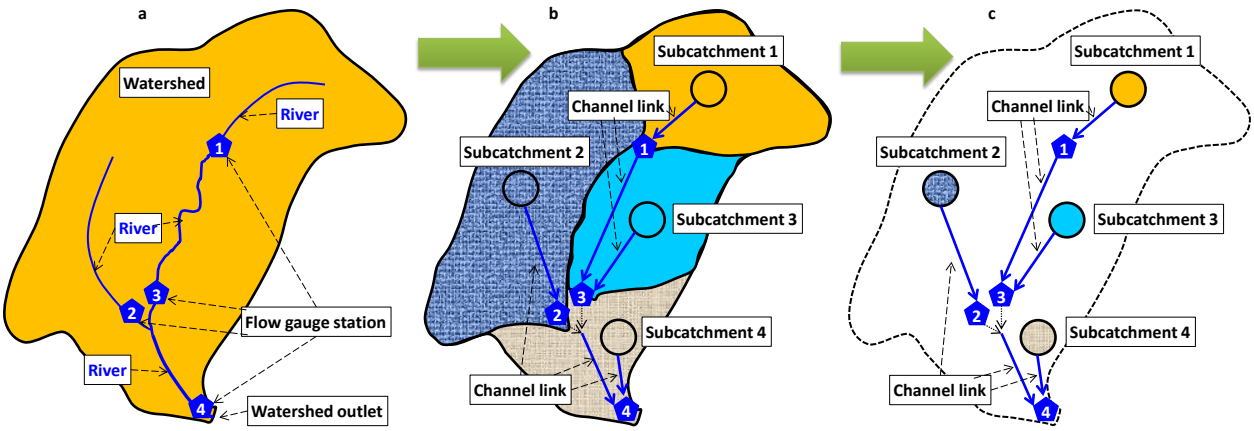

Figure 2. Process of watershed simplification and model structure.

3.2 Deriving the efficient numerical scheme for the distributed open channel routing sub-model

The core element of the real-time flood forecast model in this study is the one-dimensional, distributed open channel routing sub-model. As described in the introduction that most of the watersheds in BC are mountainous, the kinematic wave simplification of the Saint-Venant Equations is employed to govern the open channel flow in this study:

$$\begin{cases} \frac{\partial Q}{\partial x} + \frac{\partial A}{\partial t} = 0 \\ S_0 = \frac{n^2 Q^2}{A^2 R^{4/3}} \end{cases} \quad (1)$$

in which Q is the flow, x and t are the spatial and temporal coordinates respectively, A is the section area, S_0 is the friction slope, n is the Manning roughness coefficient, and R is the hydraulic radius and is given by $R = A/P$ where P is the wet perimeter.

There have been many numerical solutions to Eqs. (1). The HEC-1 (US Army Corps of Engineers, 1993) and HEC-HMS (US Army Corps of Engineers, 2000) models employed an explicit finite-difference scheme to solve the kinematic wave equations. And Chow et al. (1988) proposed a linear scheme and a nonlinear scheme kinematic wave equations. However, as Chow et al. (1988) pointed out, the linear scheme introduces dispersion of the flood wave into the solution and the degree of dispersion increases with the size of time and space steps and increments, and for the nonlinear scheme, the initial estimation of the solution of the discharge is important for the iteration convergence and one of the approaches is to use the solution from the linear scheme. In simple words, the solution of the nonlinear scheme depends on the solution of the linear schemes, in which the sizes of spatial and temporal steps are restrained. Unfortunately, the rivers of the large-scale watersheds in BC are very long, e.g., the

Fraser River is about 1400 km. Consequently, it is inevitable that a numerical scheme for flow routing in these long rivers requires large spatial and temporal steps in order to obtain time efficiency for real-time flood forecasting. Therefore, an innovated numerical scheme, in which large spatial and temporal steps are adopted without sacrificing the model accuracy, is introduced to solve Eqs. (1).

The spatial and temporal discretizing scheme is shown in Fig. 3, in which the horizontal line is the spatial axis and the vertical line is the temporal one.

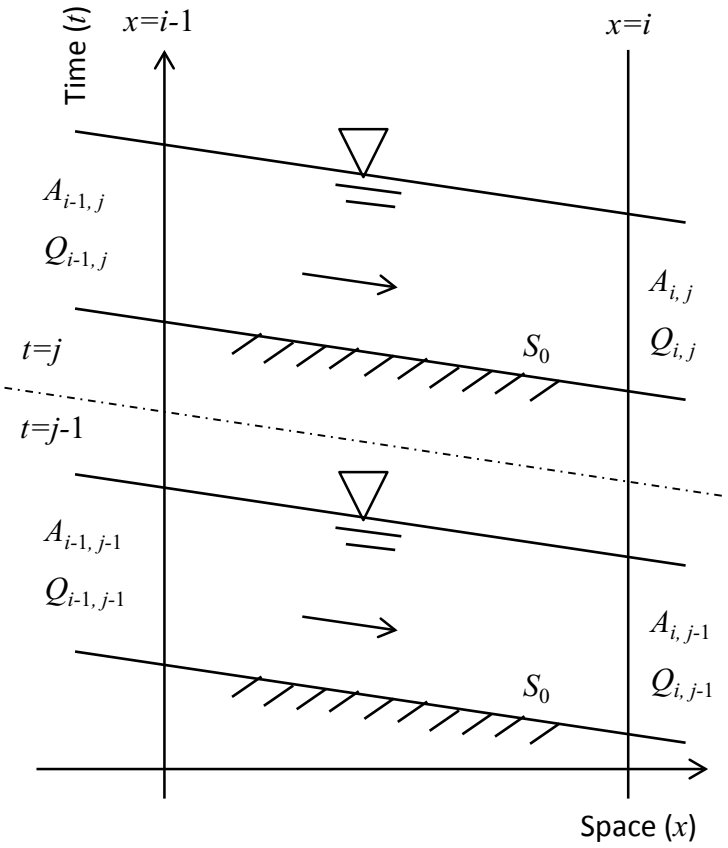

Figure 3. Spatial and temporal discretizing scheme for the one-dimensional, distributed open channel routing.

Using the temporal average forward-difference approximation for the first term and the spatial averaged forward-difference approximation for the second term, the continuity equation in Eqs. (1) becomes:

$$\frac{1}{\Delta x}\left[\frac{Q_{i,j}+Q_{i,j-1}}{2}-\frac{Q_{i-1,j}+Q_{i-1,j-1}}{2}\right]+\frac{1}{\Delta t}\left[\frac{A_{i,j}+A_{i-1,j}}{2}-\frac{A_{i,j-1}+A_{i-1,j-1}}{2}\right]=0 \quad (2)$$

in which i and j denote the spatial and temporal points on the coordinates respectively, (i,j) is the unknown node, and Δx and Δt are the spatial and temporal steps.

Discretizing and rearranging the momentum equation in Eqs. (1) produces:

$$Q_{i,j} = \frac{1}{n}\sqrt{S_0}R_{i,j}^{2/3}A_{i,j} \tag{3}$$

Assume:

$$V_{i,j} = \frac{1}{n}\sqrt{S_0}R_{i,j}^{2/3} \tag{4}$$

and substitute Eq. (4) into Eq. (3), it becomes:

$$Q_{i.j} = V_{i,j}A_{i,j} \tag{5}$$

Substituting Eq. (5) into Eq. (2) with some rearrangements gives:

$$A_{i,j} = \frac{\Delta t\left(Q_{i-1,j}+Q_{i-1,j-1}-Q_{i,j-1}\right)+\Delta x\left(A_{i,j-1}+A_{i-1,j-1}-A_{i-1,j}\right)}{\Delta t V_{i,j}+\Delta x} \tag{6}$$

If Eq. (6) is solved and $V_{i,j}$ is known, substitute $A_{i,j}$ into Eq. (5) and $Q_{i,j}$ would be solved. However, Eq. (6) is unsolvable because $V_{i,j}$ on the right-hand side is also an unknown.

In order to solve Eq. (6), an efficient scheme similar to the Semi-Implicit Method for Pressure-Linked Equations (SIMPLE) (Patankar and Spalding, 1972) is introduced. The SIMPLE is an optimized numerical scheme which solves pressure related equations iteratively with high accuracy because that it is able to avoid water balance errors and the divergence problem (Luo, 2007), and therefore this scheme was adopted to solve the diffusive-wave governing equations of the fully distributed, physics-based watershed model – LUOM (Luo, 2007). Pressure is a concept in fluid dynamics and the relevant concept in hydrology is water head or water depth (Luo, 2007). In this study, the cross section of the open channel is assumed rectangular and therefore (h is the water depth and b is the width of the channel):

$$A = bh \tag{7}$$

$$\begin{cases} P = b + 2h \\ R = A/P \end{cases} \tag{8}$$

Or in a simplified form:

$$R_{i,j} = f\left(h_{i,j}\right) \tag{9}$$

At the beginning of the iteration, the initial value of the water depth is set to the water depth of the previous time step:

$$\left(h_{i,j}\right)^{(0)} = h_{i,j-1} \tag{10}$$

Substituting Eq. (10) into Eq. (9) yields:

$$\left(R_{i,j}\right)^{(0)} = f\left(\left(h_{i,j}\right)^{(0)}\right) \tag{11}$$

Substituting Eq. (11) into Eq. (4) gives:

$$\left(V_{i,j}\right)^{(0)} = \frac{1}{n}\sqrt{S_0}\left(\left(R_{i,j}\right)^{(0)}\right)^{2/3} \tag{12}$$

With this initial value of $V_{i,j}$, Eq. (6) is rewritten as:

$$\left(A_{i,j}\right)^{(1)} = \frac{\Delta t\left(Q_{i-1,j}+Q_{i-1,j-1}-Q_{i,j-1}\right)+\Delta x\left(A_{i,j-1}+A_{i-1,j-1}-A_{i-1,j}\right)}{\Delta t\left(V_{i,j}\right)^{(0)}+\Delta x} \tag{13}$$

In these equations, superscript (0) means that the value of the variable in the parentheses before it is the initial value, and superscript (1) means that the value of the variable in the parentheses before it is the value found in the iteration step 1, and so on. If k-1 and k are used to denote the previous and the current iteration steps, the general form of the iteration equation for Eq. 6 is:

$$\left(A_{i,j}\right)^{(k)} = \frac{\Delta t\left(Q_{i-1,j}+Q_{i-1,j-1}-Q_{i,j-1}\right)+\Delta x\left(A_{i,j-1}+A_{i-1,j-1}-A_{i-1,j}\right)}{\Delta t\left(V_{i,j}\right)^{(k-1)}+\Delta x} \tag{14}$$

For iteration step k, the initial value of water depth is $\left(h_{i,j}\right)^{(k-1)}$, which can be found from Eq. (7) by substituting the result of Eq. 14 into it and after rearrangements:

$$\left(h_{i,j}\right)^{(k)} = \left(A_{i,j}\right)^{(k)}/b \tag{15}$$

The correction (h') to the initial value of water depth can be calculated as below:

$$h'_{i,j} = \left(h_{i,j}\right)^{(k)} - \left(h_{i,j}\right)^{(k-1)} \tag{16}$$

The new initial value of water depth for the next iteration step (k+1) is recalculated as shown below:

$$\left(h_{i,j}\right)^{(k)} = \left(h_{i,j}\right)^{(k-1)} + \alpha h'_{i,j} \tag{17}$$

where $\pm$is the so-called under-relaxation factor which varies from 0 to 1. Use the new $\left(h_{i,j}\right)^{(k)}$ to calculate $\left(V_{i,j}\right)^{(k)}$ and then substitute $\left(V_{i,j}\right)^{(k)}$ into the iteration Eq. (14), and so on until that h' approaches 0 or a small value of the desired accuracy.

The upstream boundary conditions and initial conditions are given by the hydrographs of upstream subcatchment nodes, which are the outputs from the lumped watershed routing sub-model described below. Because forward-difference is used to discretize the governing equations, downstream boundary conditions are not necessary. There are many lakes in BC's watersheds. Each of the lakes is routed as a single channel node by using the storage curve.

In order to test the efficiency of this numerical scheme, a sensitivity analysis for the spatial step is carried out in a 100 km long open channel by using a synthetic input hydrograph with a peak of 2415 m^3/s and the duration of 240 hours (10 days). The temporal step (Δt) is 3600 second (1 hour) and six spatial steps (Δx), 1 km, 2 km, 5 km, 10 km, 20 km and 50 km are selected to test the model. Fig. 4 is a comparison of the output hydrographs for different spatial steps at the channel outlet 100 km

downstream of the upstream boundary. The result shows that the hydrographs for spatial steps from 1 km to 20 km are almost identical, and only the hydrograph for Δx = 50 km shows some minor deviations prior to the peak. Comparing numerically with the hydrograph for Δx = 1 km, the maximum deviations for the hydrographs for Δx = 2 km, 5 km, 10 km, 20 km, and 50 km are 0%, 0%, 0.1%, 0.6% and 3.3 % respectively. From this result of the sensitivity analysis, it is safe to say that a spatial step up to 20 km can be used for this numerical scheme for simulations of high accuracy.

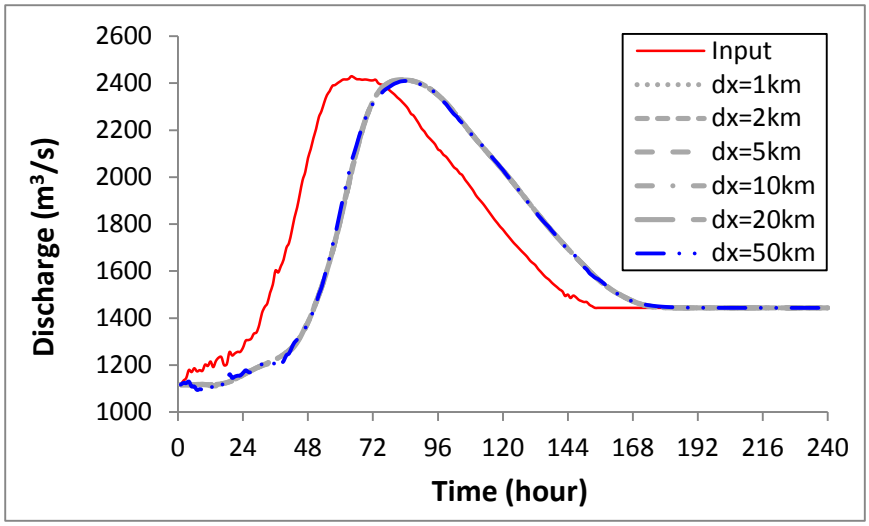

Figure 4. Comparison of output hydrographs of different spatial steps at the channel outlet 100 km downstream of the upstream boundary.

3.3 Spatial and temporal steps

Based on the discussion in the above section, the spatial step for a channel link is set to a distance between 1 km to 20 km dependent on the length of the channel link so that a channel link has as few as possible spatial grids but no fewer than two. And, in order to capture the flood peaking time in a day, an hourly time step is adopted in this study. The hourly time step is applied to both the distributed open channel routing sub-model and the lumped watershed routing sub-model, which is discussed below. All the daily climate data, observed and forecast precipitation and temperatures, are distributed into hourly series by using typical distributions derived from the historical records (Fig. 5).

3.4 Lumped watershed routing sub-module for subcatchments

As discussed in Section 3.1, in this study, a watershed is divided into a number of subcatchments, which are further simplified into a series of individual nodes. The water balance of each subcatchment is

calculated as a single node. The water balance equation is given by:

$$W = R + M + G - E - I \tag{18}$$

in which W (≥0) is the net water input to the subcatchment and has the unit of mm/hour, and this unit is used for all the terms on the right-hand side of the equation as this study employs an hourly time step, R is the rainfall, M is the snowmelt, G is the groundwater seepage to the system or the channel link which connects this subcatchment to the downstream flow gauge station, E is the evapotranspiration, and I is the infiltration to the unsaturated soil and the recharge to the groundwater.

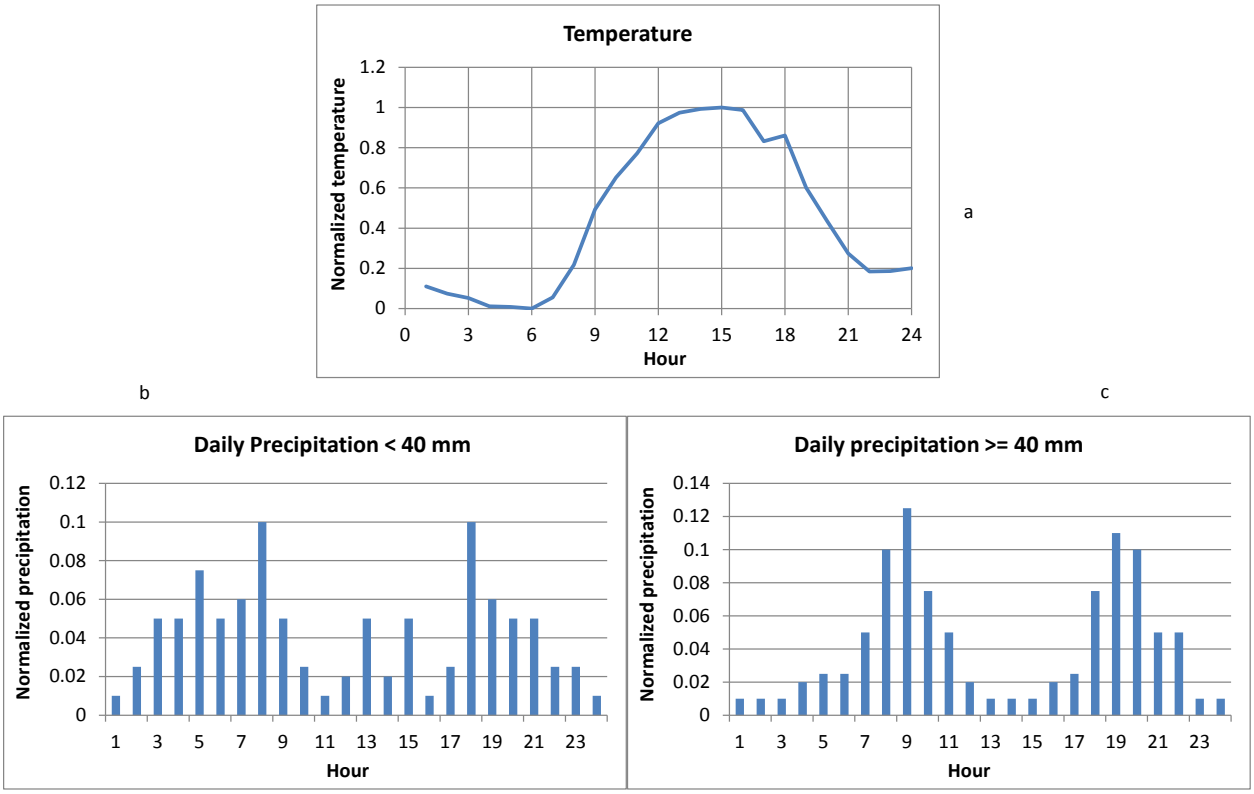

Figure 5. Distribution of daily temperature and precipitation into hourly series (a – distribution of temperature, and b and c – distribution of precipitation).

As most watersheds in BC are snow-dominated, simulating snowmelt with acceptable accuracy becomes critical for real-time flood forecasting during the snowmelt freshet season. Though the energy balance method provides a physics-based estimation of snowmelt, its extensive data requirements always frustrate its practice, and therefore, operational systems for snowmelt prediction take the temperature-index method as a substitution (Gray and Prowse, 1992). Besides the temperature-index method, the UBC Watershed Model provides a method to simulate daily snowmelt by dividing a subcatchment into several elevation bands and using the simplified energy balance method, which is driven by daily maximum and minimum temperatures, to simulate snowmelt in each of the elevation

bands (Quick and Pipes, 1977). The SWAT model (Arnold et al., 1998) proposed a temperature-index method to estimate the daily snowmelt by relating the snowmelt rate to the mean daily temperature and the snowpack temperature. Debele et al. (2009) employed one of the most commonly used temperature-index methods to estimate the daily snowmelt – the sinusoidal equation, which assumes that the potential daily snowmelt rate varies between two ranges: the maximum (assumed to occur on June 21st) and the minimum (assumed to occur on December 21st) following the sinusoidal function based on the day of the year. Debele et al. (2009) found that it is possible for the less detailed temperature-index equations to perform as equal, or sometimes even better, as the energy budget approach. Both these two temperature-index methods and other temperature-index equations depend on the mean daily temperatures to estimate the snowmelt rate.

However, this study adopts an hourly time step and therefore hourly, rather than daily, snowmelt must be estimated. Simple disaggregation of the daily snowmelt rate to the hourly rate is not working because that the existing temperature-index methods rely on the mean daily temperatures. Consequently, in order to use the temperature-index method to estimate hourly snowmelt on a subcatchment scale, an equation dependent on the hourly temperature rather than on the mean daily temperature becomes necessary. The most common expression of the temperature-index method proposed by Gray and Prowse (1992) is used as the basic form of the hourly snowmelt equation:

$$M = M_f(T_i - T_b) \tag{19}$$

where M is the snowmelt in an hour (mm/hour), M_f is the melt factor, T_i is the air temperature at the time step (hour) and T_b is the base temperature, at which snow starts to melt.

A test run of Eq. (19) in a smaller subcatchment with an hourly time step was carried out. The results showed that this equation did not sufficiently accurately estimate snowmelt. In order to obtain better estimations of snowmelt on a subcatchment scale with an hourly time step, modifications to Eq. (19) were made. In this study, the following transformation of Eq. (19) is employed to simulate the snowmelt on a subcatchment scale with an hourly time step:

$$M = c_a c_d M_f(T_i - T_b)^{\beta} \tag{20}$$

where c_a is a correction factor related to the snowpack covering area over the subcatchment, c_d is the correction factor related to the ordinal date in the year, and β has a value between 0 and 1. The snowpack covering area correction facto (c_a) is calculated every time step (hour) by comparing the snowpack area with the subcatchment area. The ordinal date correction factor (c_d) is a linear function of the ordinal date which defines the maximum and minimum snowmelt rates of the year. And c_a and c_d are subject to calibration. And β is a constant related to the size of the subcatchment and also subject to calibration. Note that Eq. (20) reduces to Eq. (19) when c_a, c_d and β are equal to 1.

Rainfall (R) is the precipitation when the average air temperature is greater than 0°C, otherwise, the precipitation will contribute to the accumulation of snow water equivalent (SWE) over the subcatchment. The evapotranspiration (E) is estimated with a simplified approach similar to the UBC

Watershed Model (Quick and Pipes, 1977). In this study, the potential evapotranspiration is calculated by timing the temperature of the time step (hour) by an evaporation constant and a monthly factor. And the infiltration and recharge to groundwater (I) is simulated with a simplified model similar to the LUOM (Luo, 2007), in which the single-layer Green-Ampt model is employed to simulate the infiltration into the upper soil before it is saturated and after that the infiltration rate reduces to the saturated hydraulic conductivity of the soil. The watershed routing sub-model stores groundwater. The groundwater model is a simplified version of the groundwater model developed by Luo (2000; 2007). And the groundwater seepage (G) to the system is calculated by timing the groundwater storage with a seepage constant, which is subject to calibration each run, and G is always greater than or equal to 0.

During the warmer part of the freshet season, in which the thaw of snow and ice has set in and the melt water can run through the overland into the channel, the net water input to the subcatchment W from Eq. (18), which is always greater than or equal to 0, can be deemed equivalent to the excess rainfall for a rainfall-dominated watershed. And therefore, the Instantaneous Unit Hydrograph (IUH) method is adopted to generate the initial channel runoff for this net water input (W) to the subcatchment node. Proposed first by Sherman (1932), the Unit Hydrograph (UH) of a watershed is defined as the direct runoff hydrograph resulted from a unit depth of excess rainfall, the net water input (W) in this study, was generated uniformly over the drainage area at a constant rate for an effective duration (Chow et al., 1988). Nash (1957) proposed a cascade of a number of linear reservoirs for a natural watershed. US Army Corps of Engineers (1980) gave and Chow et al. (1988) derived the impulse response function of a watershed with a single linear reservoir as below:

$$u(\tau) = \frac{1}{k} e^{-\tau/k} \tag{21}$$

in which u is the unit response to the impulse, $\ddot{A}$is the lag time, and k is the storage coefficient which has the unit of time and is related to watershed characteristics and to the intensity of effective rainfall (US Army Corps of Engineers, 1980). Assuming that the watershed (subcatchment) consists of a cascade of N linear reservoirs, the IUH is given by:

$$u(\tau) = \frac{t^{N-1} e^{-\tau/k}}{k^N (N-1)!} \tag{22}$$

If N is a real number rather than an integer, $(N\text{-}1)!$ becomes a gamma function of N. Eq. (22) was given by Dooge (1973) and can be derived by substituting the output from Eq. (21) as the input into the convolution integral equation proposed by Nash (1957), Chow et al. (1988) and Singh (1988), reservoir by reservoir (Ocak and Bayazit, 2003). A large number of studies, such as Nash (1957, 1959), have been carried out to estimate N and k. However, in this study, N and k are related to the subcatchment area, and $N \leq 10$ (the value varies with the subcatchment area) and $k = c\sqrt{A/A_0}$, where c is a constant subject to calibration, A is the subcatchment area and A_0 is the area normalizing factor.

The output discharge of the net water input W at time step l (W_l) is obtained by using the

following equation:

$$Q_l(t) = c_q W_l A u(t - t_{l0}) \quad (23)$$

in which c_q is a constant subject to calibration, t is the time, t_{l0} is the time when the net water input (W_l) occurs and $\tau = t - t_{l0}$. The total discharge at time t from all water inputs prior to t is given by:

$$Q(t) = \sum_{l=1}^{L} Q_l(t) \quad (24)$$

where L is the total number of water inputs which have a non-zero output from the IUH at time t. Eq. (24) provides the upstream boundary and initial conditions to the one-dimensional, distributed open channel routing sub-model.

3.5 Operational settings

For modeling efficiency in computing time, the modeling period is set to 30 days, which means that the model only runs a 30-day period, the first 20 days for the model calibration and the last 10 days for the forecast. This does not mean that the model can only produce a 30-day hydrograph but rather means that the model parameters are maintained constant for a time span of 30 days. The model may start running at any time of the year and the intermediate values of all model variables are recorded in a temporary file at the end of each day of the 30-day period. Later, the model can be picked up and rerun again any day within the 30-day period to resume the simulation and produce a new and consecutive hydrograph which smoothly connects to the previous one at the time point when the model resumes running (Fig. 6).

In this study, the 10-day forecast hydrograph starts from the latest hour of the current day, at which the provisional observation flow data has arrived. It is usually difficult to match perfectly the simulated and observed flows at a specific point of time through model calibration. In order to generate the 10-day forecast hydrograph which starts from the latest observed flow (the first forecast flow is equal to the observed flow), the simulated hydrograph has to be shifted by a constant increment which is the simulation bias at this time point. This is also shown in Fig. 6.

Some of the subcatchments are regulated, for which no watershed routing or channel routing is carried out. For the regulated subcatchments, the 10-day forecast hydrograph is generated by extending the trend of the daily flow of the 19th and 20th days. The observed flow for the early 20-day calibration period and the later 10-day forecast flow constitute a 30-day hydrograph, which is the input to the downstream channel link and is routed downstream to the watershed outlet through the channel link network.

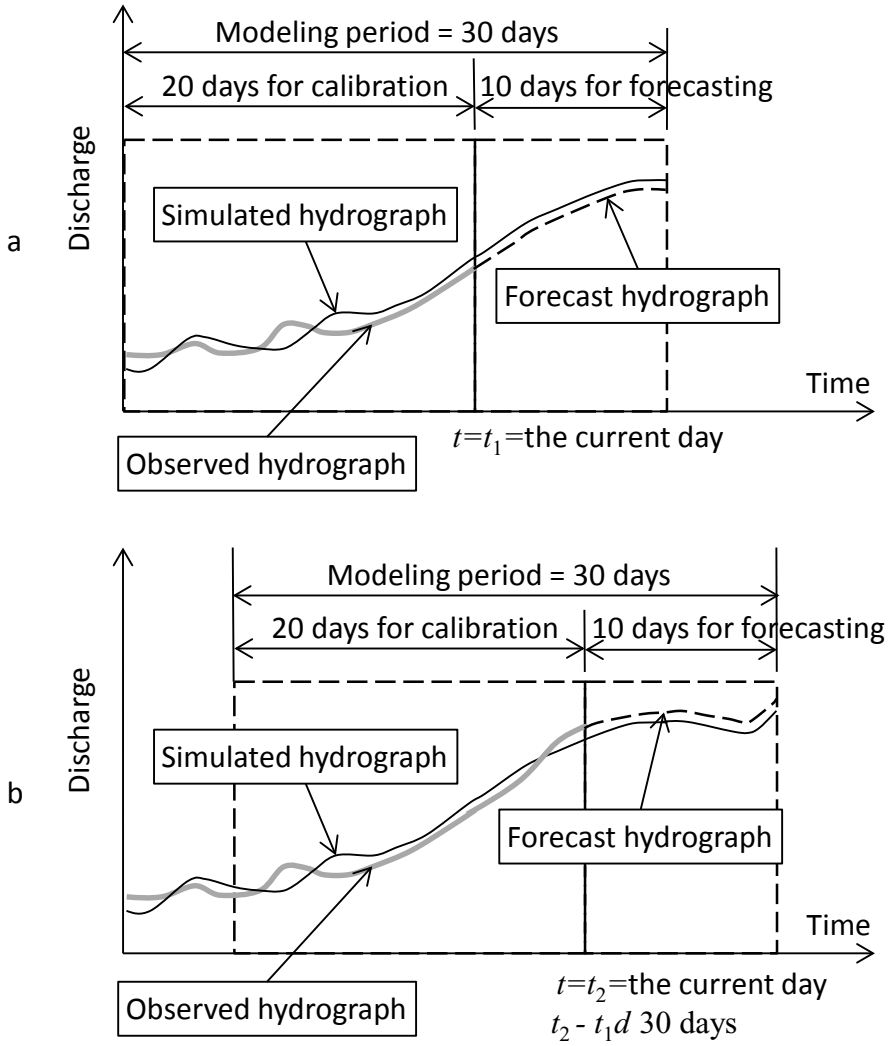

Figure 6. Model operational settings – model runs a 30-day period and moves on day by day or at an interval shorter than 30 days.

4. Results and discussion

The model was first developed in 2013 for the Fraser River watershed in BC. It has been tested intensively and improved substantially over the past three years. At the current stage (2015) of this study, the modelled area has been expanded from the Fraser River to a total of 71 subcatchments which are distributed over all the seven major watersheds in BC listed in Table 1 and cover an area of 583,400 km^2, or 61.5% of the province's land area (Fig. 7). A subcatchment is so defined that a WSC flow gauge station is located at its outlet (shown in Fig. 7) to facilitate the model calibration for the subcatchment.

Fig. 7 also shows all the climate stations, at which automated data are available, including EC climate stations, Fire Weather stations and ASP. It can be seen from Fig. 7 that some of the subcatchments protrude through provincial or international boundaries. One run of the model for the total 71 subcatchments over a 30-day period consumes 8 minutes of computing time on a computer of 2.6 GHz CPU clock. If the modeling starts at 9 am and the forecasts are issued at noon each day, there are a total of 3 hours available for modelling which is sufficient for model calibration for many times and time for the other forecasting operations as well.

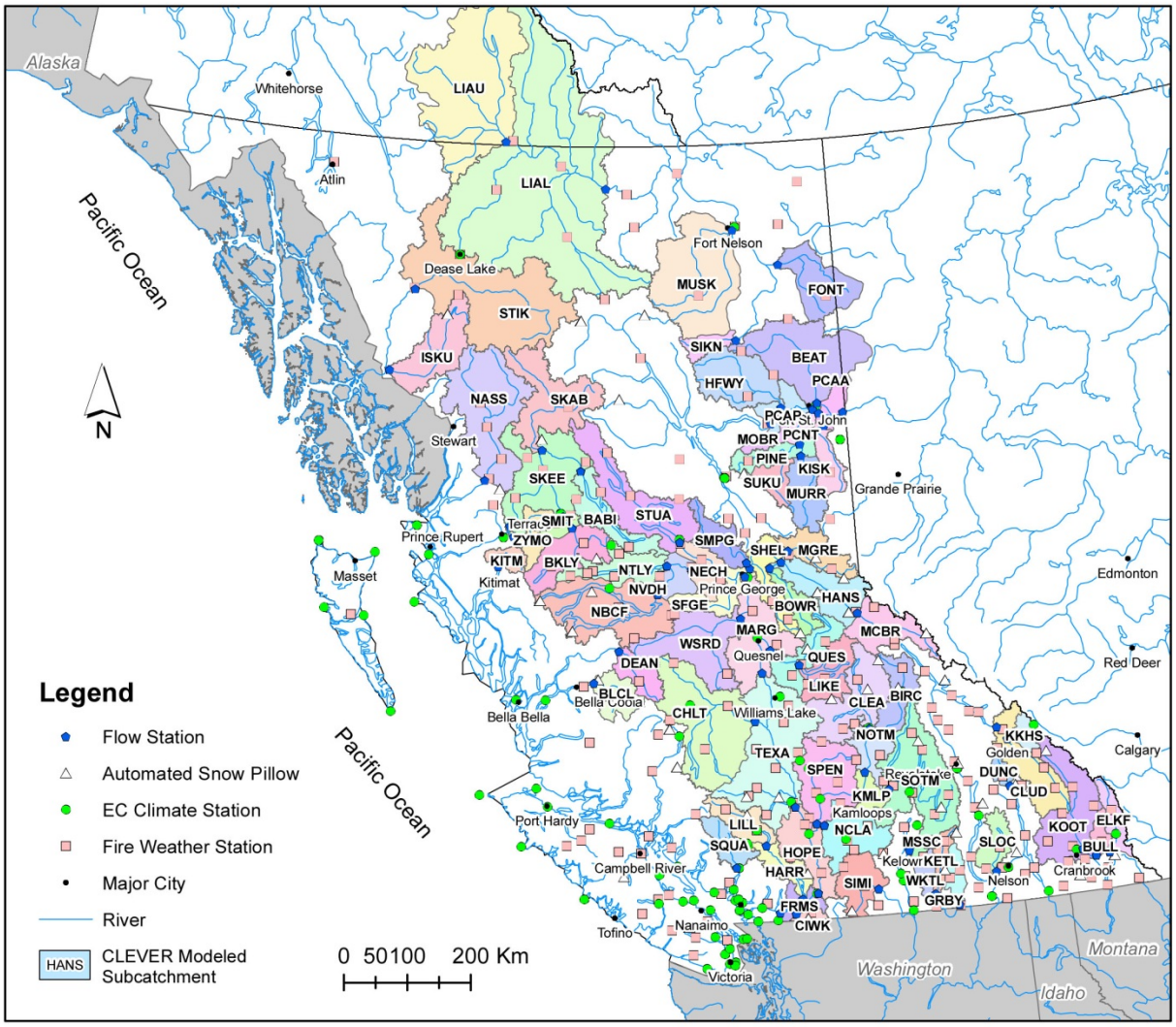

Figure 7. Seventy one (71) subcatchments currently covered by the model.

4.1 Model calibration

According to Nash and Sutcliffe (1970), the model forecast accuracy is best assessed by retrospective comparison of forecast actual made and the observed values during the forecast period. The 10-day forecast climate data from the CMC NWP Model became technically available for this study in 2015, and the model expanded its forecasts from 5 days to 10 days. Consequently, the results from the model's testing run in 2015 are used to evaluate the model's performance. The test run was actually carried out during 2015 freshet season, day by day, except some weekends and holidays and the results were posted for use by internal staff. Although the model actually started running from January 1, 2015, only the outputs from March 1, 2015, which was the early onset of 2015 spring, to July 20, 2015, when this manuscript was prepared, are used for the model performance evaluation. During this warm spring and summer period, the flow gauge stations tend to function better and therefore provide provisional observed flow data with higher accuracy than during the freezing winter. The model produces two categories of results for each flow gauge station, the simulated hydrograph from model calibration and a series of 10-day forecast hydrographs which are generated each day when the model was running. Fig. 8 shows the outputs of these two categories of results for the WSC station – Fraser at Hope (08MF005) and Fig. 9 shows an example of the posted forecast for this station.

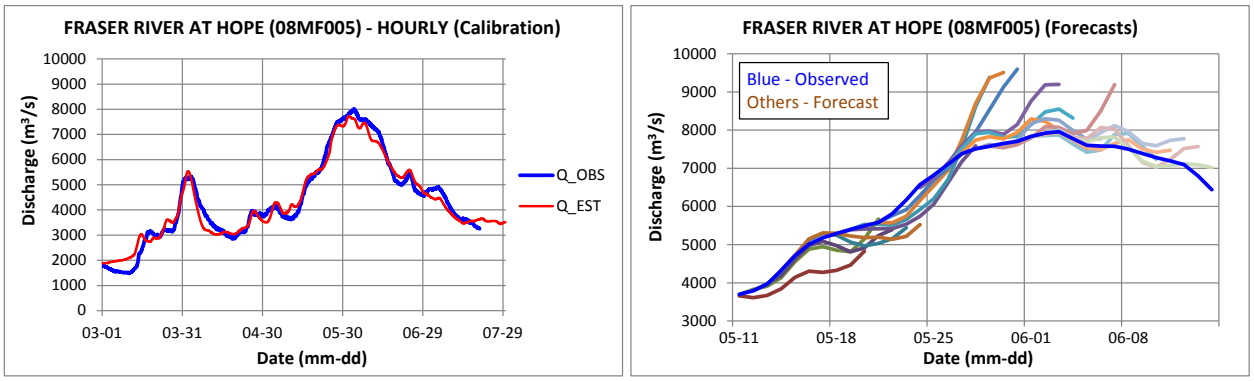

a b

Figure 8. Model outputs at station Fraser at Hope (08MF005) – calibration hydrograph (a) and forecast hydrographs (b).

Evaluation of the model calibration, which means the comparison of the simulated hydrograph from the calibration and the observed hydrograph, was primarily carried out visually during the freshet season and statistically later by using the coefficient of model efficiency (C_e), the coefficient of determination (C_d) and the percentage volume difference (dV) (Nash and Sutcliffe, 1970). The coefficient of model efficiency (C_e) describes how well the volume and timing of the simulated hydrograph compares to the observed hydrograph and is given by:

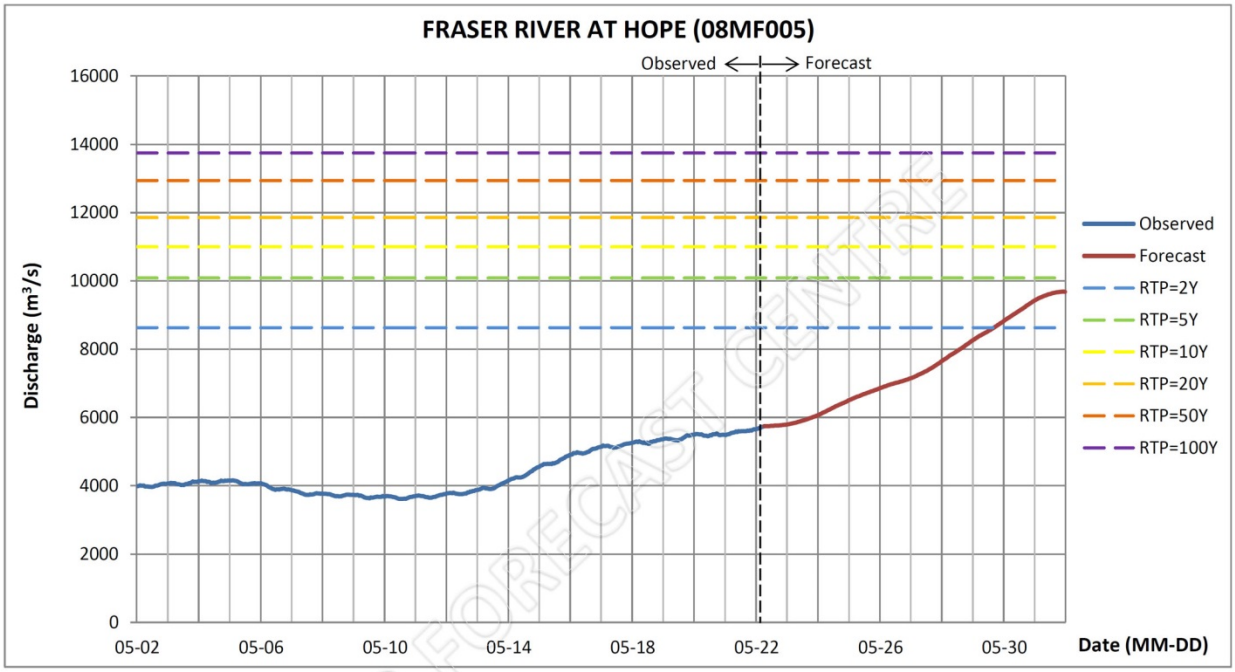

Reading at 7AM (m^3/s)	Forecast Daily Discharge (m^3/s): MAX / AVERAGE / MIN									
Fri	Fri	Sat	Sun	Mon	Tue	Wed	Thu	Fri	Sat	Sun
2015-05-22	2015-05-22	2015-05-23	2015-05-24	2015-05-25	2015-05-26	2015-05-27	2015-05-28	2015-05-29	2015-05-30	2015-05-31
5718	5792	6061	6492	6848	7143	7635	8247	8811	9416	9684
	5759	**5914**	**6288**	**6684**	**7005**	**7374**	**7952**	**8536**	**9125**	**9599**
	5744	5798	6078	6509	6863	7158	7662	8273	8837	9438

Colour Scheme for Return Periods: 1-Yr | 2-Yr | 5-Yr | 10-Yr | 20-Yr | 50-Yr | 100-Yr

Note: Both observed and forecast data are hourly averages. The observed data is provisional as it is from Water Survey Canada. When missing data are present in the observed data series, methods such as interpolation, extrapolation and referring to the rating curve are involved to connect and/or extend the data.

Figure 9. Example of test forecast for Fraser at Hope (08MF005) released on May 22, 2015.

$$C_e = 1 - \frac{\sum_{j=1}^{m}\left(Q_{obs}^{j} - Q_{sim}^{j}\right)^2}{\sum_{j=1}^{m}\left(Q_{obs}^{j} - \overline{Q_{obs}}\right)^2} \tag{25}$$

where $\overline{Q_{obs}}$ is the mean of the observed flow and is given by:

$$\overline{Q_{obs}} = \frac{1}{m}\sum_{j=1}^{m} Q_{obs}^{j} \tag{26}$$

in which m is the total number of time steps, Q_{obs}^{j} is the observed flow at time step j, and Q_{sim}^{j} is the simulated flow at time step j. The coefficient of determination (C_d) measures how well the shape of the simulated hydrograph reflects the observed hydrograph and depends solely on the timing of changes in the hydrograph. If the mean of the simulated flow ($\overline{Q_{sim}}$), the product mean of the observed and simulated flows ($\bar{P}$), the mean of the squared observed flow ($\overline{Q_{obs}^2}$), the mean of the squared simulated flow ($\overline{Q_{sim}^2}$) are given by:

$$\overline{Q_{sim}} = \frac{1}{m}\sum_{j=1}^{m} Q_{sim}^{j} \tag{27}$$

$$\bar{P} = \frac{1}{m}\sum_{j=1}^{m}\left(Q_{obs}^{j} \cdot Q_{sim}^{j}\right) \tag{28}$$

$$\overline{Q_{obs}^{2}} = \frac{1}{m}\sum_{j=1}^{m}\left(Q_{obs}^{j}\right)^{2} \tag{29}$$

$$\overline{Q_{sim}^{2}} = \frac{1}{m}\sum_{j=1}^{m}\left(Q_{sim}^{j}\right)^{2} \tag{30}$$

C_d can be written as:

$$\begin{cases} C_d = 1 - \dfrac{\sum_{j=1}^{m}\left[Q_{obs}^{j} - \left(a \cdot Q_{sim}^{j} + b\right)\right]^2}{\sum_{j=1}^{m}\left(Q_{obs}^{j} - \overline{Q_{obs}}\right)^2} \\ a = \left(\bar{P} - \overline{Q_{obs}} \cdot \overline{Q_{sim}}\right) / \left(\overline{Q_{sim}^{2}} - \overline{Q_{sim}}^{2}\right) \\ b = \overline{Q_{obs}} - a \cdot \overline{Q_{sim}} \end{cases} \tag{31}$$

And the percentage volume difference (dV) is calculated by:

$$dV = 100 \times \left(\overline{Q_{sim}} - \overline{Q_{obs}}\right) / \overline{Q_{obs}} \tag{32}$$

The closer the values of C_e and C_d are to 1 and the value of dV to 0%, the more successful the model is calibrated. Table 2 and Fig. 10 show the statistics about C_e, C_d and dV of the model calibration for the total 71 stations or subcatchments.

Table 2. Statistics of model calibration for the total 71 stations (2015)

Calibration	Ce		Cd		|dV|		
	Count	%	Count	%	Calibration	Count	%
0.95~1.00	17	24	18	25	<=1%	19	27
0.90~0.95	13	18	14	20	5%~1%	29	41
0.85~0.90	9	13	9	13	10%~5%	13	18
0.80~0.85	9	13	10	14	15%~10%	6	8
Subtotal	48	68	51	72	Subtotal	67	94
0.70~0.80	8	11	8	11	20%~15%	2	3
0.60~0.70	6	8	5	7	25%~20%	1	1
0.50~0.60	2	3	3	4	30%~25%	1	1
<0.50	7	10	4	6	>30%	0	0
Subtotal	23	32	20	28	Subtotal	4	6
Total	71	100	71	100	Total	71	100

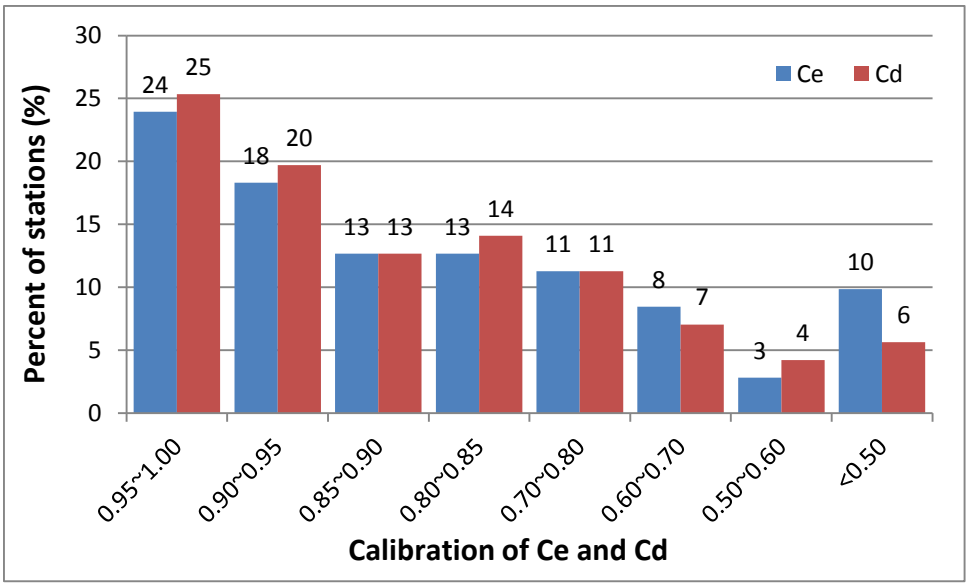

a

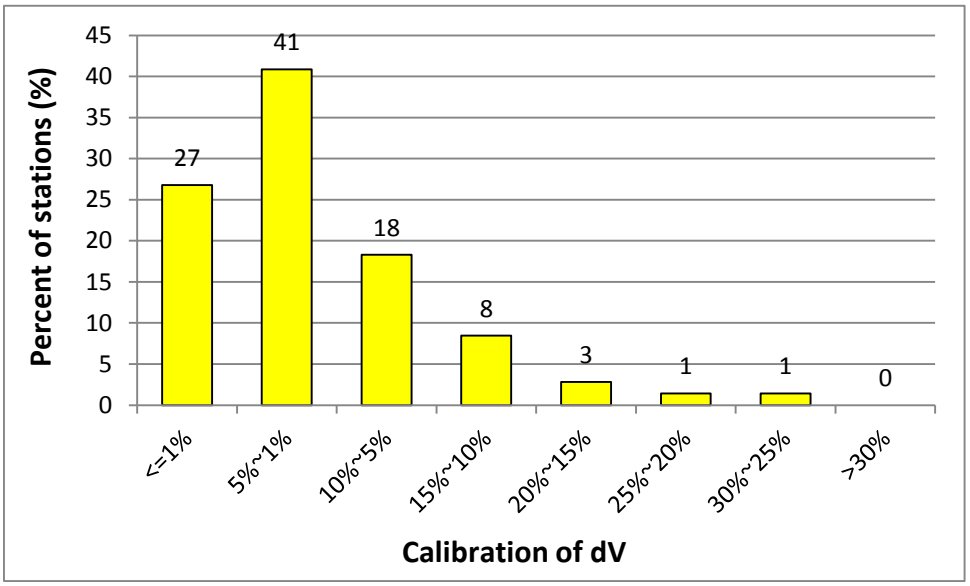

b

Figure 10. Statistics of C_e, C_d and dV of model calibration for total 71 stations.

It can be seen that, for the total 71 stations, 68% or 48 stations have a value of C_e greater than or equal to 0.8, 72% or 51 stations have a value of C_d greater than or equal to 0.8 and 94% or 67 stations have a value of dV smaller or equal to 15%. These statistical results demonstrate that the model was well calibrated at most of the stations. Table 3 shows the model calibration at the selected 13 key stations over the 7 major watersheds in BC.

Table 3. Model calibrations at 13 selected key stations (2015)

Watershed	Station Name and ID	Ce	Cd	dV (%)
Fraser	Fraser River at Shelley (08KB001)	0.86	0.88	-6.1
	Quesnel River near Quesnel (08KH006)	0.97	0.97	-2.4
	Thompson River near Spences Bridge (08LF051)	0.97	0.98	2.7
	Fraser River at Hope (08MF005)	0.97	0.97	-0.2
Columbia	Columbia River at Donald (08NB005)	0.96	0.96	1.1
	Kootenay River at Fort Steele (08NG065)	0.93	0.94	-1.1
Skeena	Bulkley River at Quick (08EE004)	0.96	0.97	-0.8
	Skeena River at Usk (08EF001)	0.97	0.97	-1.7
Nass	Nass River above Shumal Creek (08DB001)	0.93	0.95	3.0
Stikine	Stikine River at Telegraph Creek (08CE001)	0.93	0.95	-7.8
Liard	Liard River at Lower Crossing (10BE001)	0.96	0.96	0.7
Peace	Pine River at East Pine (07FB001)	0.81	0.82	2.0
	Peace River above Alces River (07FD010)	0.62	0.81	14.7

The model was well calibrated in most of the watersheds except the Peace River especially at the station of Peace River above Alces River (07FD010). The major reason is that the number of climate stations located in this watershed is fewer than in other watersheds across the province and therefore the representativeness of the climate stations is lower. The other reason may be the errors in provisional observed flow data. The underestimation of water volume at Stikine River at Telegraph Creek (08CE001) is also likely the result of fewer climate stations located in the watershed. The model calibration at Fraser River at Shelley (08KB001) is good enough but is not as good as other stations, and this is probably because of both the representativeness of the climate stations and errors in the provisional observed flow data during the early spring.

The above modeling calibration results were obtained from 2015, which was an intermediate water year. The provisional instantaneous peak flow recorded at the WSC station - Fraser River at Hope (08MF005) was 8119.903 m^3/s (at 2015-06-03 9:55am). The year of 2012 was a relatively high water year and the instantaneous peak flow recorded at the same station was 11900 m^3/s (at 2012-06-22 9:51am). The climate data for the Fraser River watershed are available for 2012 and so the model was run for the 4 Fraser River subcatchments for that year (as shows in Table 3) to verify the model calibration. The verification results are given in Table 4, which shows that the model can also be well calibrated at all the 4 stations during the high water year (2012).

Table 4. Model verification in the Fraser in a high water year (2012)

Watershed	Station Name and ID	Ce	Cd	dV(%)
Fraser	Fraser River at Shelley (08KB001)	0.96	0.96	0.6
	Quesnel River near Quesnel (08KH006)	0.97	0.98	0.7
	Thompson River near Spences Bridge (08LF051)	0.99	0.99	0.5
	Fraser River at Hope (08MF005)	0.98	0.99	-1.3

4.2 Model forecasts

The accuracy of the 10-day forecast flows is evaluated statistically after the freshet and only when all of the observed flow data have become available by using the following equations of the relative mean absolute error (E_{ra}) and the square of the Pearson product moment correlation coefficient between the forecast and observed flows – r squared (r^2):

$$E_{ra} = 100 \times \left(\frac{1}{m}\sum_{j=1}^{m}\left|Q_{sim}^{j} - Q_{obs}^{j}\right|\right)/\overline{Q_{obs}} \tag{33}$$

$$r^2 = \frac{\left[\sum_{j=1}^{m}\left(Q_{obs}^{j}-\overline{Q_{obs}}\right)\left(Q_{sim}^{j}-\overline{Q_{sim}}\right)\right]^2}{\sum_{j=1}^{m}\left(Q_{obs}^{j}-\overline{Q_{obs}}\right)^2 \sum_{j=1}^{m}\left(Q_{sim}^{j}-\overline{Q_{sim}}\right)^2} \tag{34}$$

The closer the value of E_{ra} is to 0% and the value of r^2 is to 1, the better the forecast is. The largest value of r^2 (1.0) can be achieved for cases where there is a constant bias in the forecasts and must be used with care (Lettenmaier and Wood, 1992). However, in this study, the forecast hydrograph is generated by shifting the simulated hydrograph for the 10-day forecast period by a constant increment (bias), and therefore r^2 is an appropriate indicator of the correctness of the trend of the forecast hydrograph. Table 5 shows the statistics about E_{ra} and r^2 of the 10-day forecasts for the total 71 stations or subcatchments over the entire evaluation period (March 1 to July 20, 2015) and the period of peak flows (May 11 to June 11, 2015).

Table 5. Statistics of the 10-day forecasts for the total 71 stations (2015)

Era					r squared				
Forecast	Mar.01 - Jul.20		May 11 - Jun.11		Forecast	Mar.01 - Jul.20		May 11 - Jun.11	
	Count	%	Count	%		Count	%	Count	%
<=10%	11	15	13	18	>=0.9	0	0	0	0
20%~10%	17	24	14	20	0.8~0.9	1	1	4	6
30%~20%	25	35	24	34	0.7~0.8	2	3	9	13
Subtotal	53	75	51	72	0.6~0.7	11	15	5	7
40%~30%	12	17	12	17	0.5~0.6	4	6	11	15
>40%	6	8	8	11	<0.5	53	75	42	59
Total	71	100	71	100	Total	71	100	71	100

It can be seen from Table 5 that the majority (75% or 53 stations over the entire evaluation period, March 1 to July 20, 2015, and 72% or 51 stations over the peaking period, May 11 to June 11, 2015) of the 71 stations have a relative mean absolute error (E_{ra}) smaller or equal to 30%. However, the majority (75% or 53 stations over the entire evaluation period and 59% or 42 stations over the peaking period) of the 71 stations have a Pearson product moment correlation coefficient (r^2) smaller than 0.5. These results suggest that the trend of the streamflow could be very difficult to forecast. Table 6 shows the E_{ra} and r^2 at the selected 13 key stations over the 7 major watersheds in BC. It can be seen from Table 6 that the values of E_{ra} of all the 13 stations for the entire evaluation period and 12 stations for the peaking period are smaller than 30% and the values of r^2 of most of the 13 stations for the peaking period are greater than or equal to 0.5. One of the most important stations among these 13 stations is Fraser River at Hope (08MF005), which is located on the northeastern boundary of the Lower Mainland including Metro Vancouver – the most populated region of the province of BC. The forecast error (E_{ra}) is 10% and 6% for the entire evaluation period and the peaking period respectively, and the correlation coefficient between the forecast and observed flows (r^2) is 0.61 and 0.74 for the entire evaluation period and the peaking period respectively. These values demonstrate that the accuracy of the forecast at Fraser River at Hope (08MF005) is relatively high.

Table 6. 10-day streamflow forecasts at 13 selected key stations (2015)

		Mar.01 - Jul.20		May 11 - Jun.11	
Watershed	Station Name and ID	Era (%)	r squared	Era (%)	r squared
Fraser	Fraser River at Shelley (08KB001)	19	0.46	16	0.52
	Quesnel River near Quesnel (08KH006)	13	0.53	14	0.71
	Thompson River near Spences Bridge (08LF051)	8	0.63	7	0.70
	Fraser River at Hope (08MF005)	10	0.61	6	0.74
Columbia	Columbia River at Donald (08NB005)	14	0.35	17	0.44
	Kootenay River at Fort Steele (08NG065)	20	0.33	24	0.42
Skeena	Bulkley River at Quick (08EE004)	18	0.39	17	0.50
	Skeena River at Usk (08EF001)	17	0.42	15	0.52
Nass	Nass River above Shumal Creek (08DB001)	24	0.38	24	0.50
Stikine	Stikine River at Telegraph Creek (08CE001)	26	0.38	41	0.51
Liard	Liard River at Lower Crossing (10BE001)	10	0.66	13	0.85
Peace	Pine River at East Pine (07FB001)	28	0.43	21	0.49
	Peace River above Alces River (07FD010)	22	0.29	21	0.40

4.3 Discussion

It must be noted that all the forecasts evaluated above were real-time forecasts and produced before the actual flows happened with forecast climate data as the model input. And therefore, the forecast errors are the combined results of four sources: 1) errors in the forecast climate data, 2) errors in the provisional flow data, 3) model's systematic errors, and 4) errors from the model calibration. The errors in the forecast climate data, which consist of the initial errors and the downscale errors, are fed into the model with the input data, then propagated in the model and finally incorporated in the model output. The provisional flow data comprises the baseline for model calibration and calculation of forecast errors, and therefore the errors in the provisional flow data are directly part of the forecast errors. The model's systematic errors are incurred by the simplification of the watershed and the governing equations and can be diminished by careful selection of model parameters through model calibration. The errors from the model calibration depend on the modeller's experience and efforts to calibrate the model. Given the fact that the model was well calibrated by using the observed climate data as model input and by using the provisional flow data as the baseline but nevertheless the accuracy of the model forecasts is not as high as the calibration, it is clear that the accuracy (initial and downscale) of the forecast climate data, especially for the longer term (4 to 10 days) plays an important role in the model forecast accuracy.

The effects of model forecast errors incurred by the errors (initial and downscale) of forecast climate data can be diminished partly by updating the model forecasts frequently by using the latest updated forecast climate data. This was the approach used in the operation of the model during 2015 freshet season. Most of the time, the model was run once a day and the forecasts were updated daily. Each run of the model generated a 10-day forecast hydrograph for each station and a number of forecast hydrographs were generated for the same station after several days of running of the model. These were not ensemble streamflow predictions (ESP) using ensemble prediction systems (EPS), which operational and research flood forecasting systems around the world are increasingly using (Cloke and Pappenberger, 2009). However, these forecast hydrographs from the model output for a number of days resemble ESP to some extent. Fig. 11 shows an example of these forecasts at the WSC station - Fraser River at Hansard (08KA004). From Fig. 11, it can be seen that the forecast hydrographs which were generated on May 20, 21 and 22, 2015 over-forecasted the flow from May 27 to 29, 2015 considerably because that the downscaled forecast climate data overestimated the temperature by 5°C to 12°C at the location of the ASP – Dome Mountain (1A19P) on May 24, 25 and 26, 2015. However, it can be seen from Fig. 11 that the forecasts generated on May 26, 2015 and later improved considerably by using the forecast climate data updated on these days.

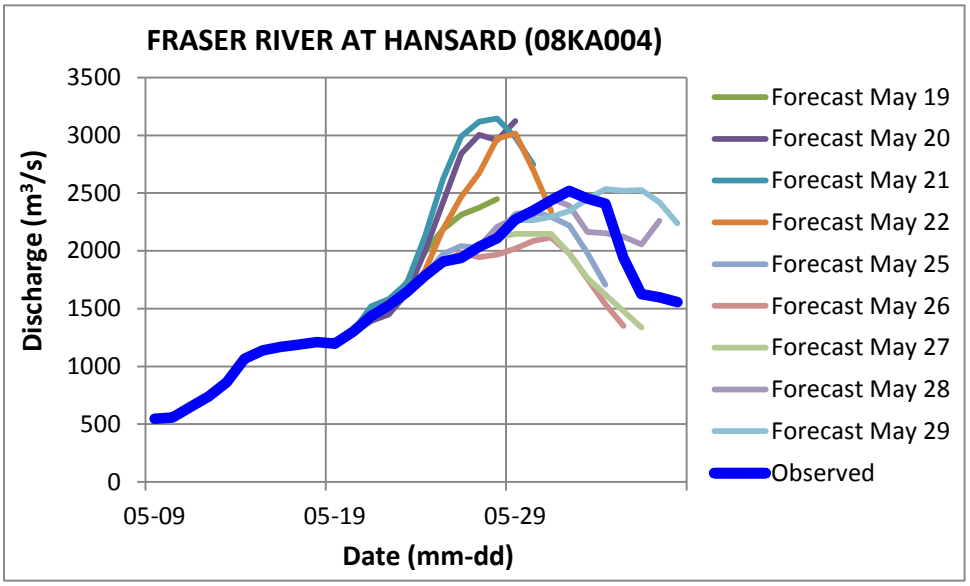

Figure 11. Example of forecasts updated on 9 days at Fraser River at Hansard (08KA004)

5. Conclusions

Based on the above description, derivation, evaluation and discussion, it can be concluded that a) the innovative numerical scheme similar to the SIMPLE is very efficient in solving the kinematic wave equations for open channel routing by using a very large spatial step up to 20 km, b) the modified temperature-index equation is valid for hourly snowmelt estimation on a subcatchment scale, and c) the Channel Links Evolution Efficient Routing (CLEVER) Model is an efficient real-time flood forecasting model for the large-scale watersheds in British Columbia with acceptable accuracy.

6. Acknowledgements

The author thanks Wenda Mason, supervisor of BC River Forecast Centre, for her full support and highly appreciates her valuable comments on the manuscript. The author also thanks all staff members of BC River Forecast Centre, David Campbell, Tobi Gardner, Tony Botica (former member) for their support in all aspects during the model development and tests.

7. References

Aral, M.M., Gunduz, O., 2006. Chapter 4 Large-scale hybrid watershed model, in: Singh, V.P., Frevert, D.K., (Eds.), Watershed Models. CRC Press, Taylor & Francis Group, Boca Raton, pp. 75-96.

Arnold, J.G., Srinivasan, R., Muttiah, R.S., Williams, J.R., 1998. Large area hydrologic modeling and assessment, Part I: model development. J. of American Water Res. Ass. 34(1), 73-89.

B.C. Ministry of Forests, Mines and Lands, 2010. The State of British Columbia's Forests, 3rd ed. Forest Practices and Investment Branch, Victoria, B.C., www.for.gov.bc.ca/hfp/sof/index.htm#2010_report

Cannings, S., Nelson, J., Cannings, R., 2011. Geology of British Columbia, new edition. Greystone Books, Vancouver.

Chau, K.W., Wu, C.L., Li Y.S., 2005. Comparison of several flood forecasting models in Yangtze River. Journal of Hydrologic Engineering, ASCE, 10(6), 485-491.

Chiang, Y., Hsu, K., Chang, F., Hong, Y., Sorooshian, S., 2007. Merging multiple precipitation sources for flash flood forecasting. Journal of Hydrology 340, 183–196.

Chow, V.T., Maidment, D.R., Mays, L.W.,1988. Applied Hydrology. McGraw-Hill, New York.

Cloke, H.L., Pappenberger, F., 2009. Ensemble flood forecasting: A review. Journal of Hydrology 375, 613–626

Dalichow, F., 1972. Agricultural Geography of British Columbia. Versatile Pub. Co., Vancouver.

Debele, B., Srinivasan, R., Gosain, A.K., 2009. Comparison of process-based and temperature-index snowmelt modeling in SWAT. Water Resour. Manage., DOI 10.1007/s11269-009-9486-2.

Environment Canada, 2010. Canadian Climate Normals 1981-2010 Station Data, http://climate.weather.gc.ca/climate_normals/index_e.html, (last access: July 02, 2015).

Estupina-Borrell, V., Dartus. D., Ababou, R., 2006. Flash flood modelling with the MARINE hydrological distributed model. Hydrology and Earth System Sciences 3, 3397–3438.

Foody, G.M., Ghoneim, E.M., Arnell, N.W., 2004. Predicting locations sensitive to flash flooding in an arid environment. Journal of Hydrology 292, 48–58.

Foster, H.D., 2001. Chapter 3 Landforms and natural hazards, in: Wood, C.J.B. (Ed.), British Columbia, the Pacific Province: Geographical Essays, Department of Geography, University of Victoria, pp. 27-44.

Gray, D.M., Prowse, T.D., 1992. Chapter 7 Snow and Floating ice, in: Maidment, D.R. (Ed.), Handbook of Hydrology, McGraw-Hill Inc., pp. 7.1-7.58.

Hapuarachchi, H.A.P., Wang, Q.J., Pagano, T. C., 2011. A review of advances in flash flood forecasting. Hydrol. Process. 25, 2771–2784.

Hare, K., Thomas, J., 1974. Climate Canada. John Wiley, Toronto.

Hopson, T., Webster, P., 2010. A 1–10 day ensemble forecasting scheme for the major river basins of Bangladesh: forecasting severe floods of 2003–2007. Journal of Hydrometeorology 11, 618-648.

Lettenmaier, D.P., Wood, E.F., 1992. Chapter 26 Hydrologic forecasting, in: Maidment, D.R. (Ed.), Handbook of Hydrology, McGraw-Hill Inc., pp. 26.1-26.30.

Luo, Q. 2000. A distributed water balance model in large-scale complex watersheds (LCW) and its application to the Kanto region, Ph.D. dissertation, Department of Civil Engineering, the University of Tokyo, Japan.

Luo, Q., 2007. A distributed surface flow model for watersheds with large water bodies and channel loops. Journal of Hydrology 337, 172–186.

Lyons, R. O., 1976. The SIMPAK program, application to simplified streamflow forecasting. Proceedings of the 44th Annual Western Snow Conference, April 1976, 87-93.

McGillivray, B., 2005. Geography of British Columbia, People and Landscapes in Transition, second ed. UBC Press, Vancouver & Toronto.

Nash, J. E., 1957. The form of the instantaneous unit hydrograph. International Association of Scientific Hydrology Publication, 45(3), 114-121.

Nash, J. E., 1959. Synthetic determination of unit hydrograph parameters. J. Geophys. Res., 64(1), 111–115.

Nash, J.E., J.V. Sutcliffe, 1970. River flow forecasting through conceptual models, 1. A discussion of principles. Journal of Hydrology 10, 282-290.

Ocak. A., Bayazit, M., 2003. Linear reservoirs in series model for unit hydrograph of finite duration. Turkish J. Eng. Env. Sci. 27, 107–113.

Patankar, S.V., Spalding, D.B., 1972. A calculation procedure for heat, mass and momentum transfer in three-dimensional parabolic flows. International Journal of Heat Mass Transaction 15, 1787–1806.

Patrick, S., 2002. The future of flood forecasting. Bulletin of the American Meteorological Society, p. 183.

Penning-Rowsell, E., Tunstall, S., Tapsell, S., Parker, D., 2000. The benefits of flood warnings: real but elusive, and politically significant. Journal of the Chartered Institution of Water and Environmental Management 14, 7–14.

Quick, M.C., Pipes, A. 1972. Daily and seasonal forecasting with a water budget model. Role of Snow and Ice in Hydrology, Proceedings of the UNESCO/WMO/IAHS Symposium, Banff, September 1972, IAHS Publ. no. 106, 1017-1034.

Quick, M.C., Pipes, A., 1975. Nonlinear channel routing by computer. ASCE Journal of the Hydraulics Division, 101 (6), 651-664.

Quick, M.C., Pipes, A., 1977. U.B.C. Watershed Model. Hydrological Sciences Bulletin, 22:1, 153-161.

Sahoo, G.B., Ray, C., De Carlo, E.H., 2006. Use of neural network to predict flash flood and attendant water qualities of a mountainous stream on Oahu, Hawaii. Journal of Hydrology 327, 525–538.

Sherman, L. K., 1932. Streamflow from Rainfall by the Unit Graph Method. Eng. News Rec. 108, 501-505.

Singh, V.P., 1988. Hydrologic Systems, Vol 1: Rainfall-Runoff Modeling. Prentice Hall, Englewood Cliffs, New Jersey.

Singh, V.P., 2012. Chapter 1 Watershed modeling, in: V.P. Singh (Ed.), Computer Models of Watershed Hydrology. Water Resources Publication, pp. 1-20.

Sirdas, S., Sen, Z., 2007. Determination of flash floods in Western Arabian Peninsula. Journal of Hydrologic Engineering 12(6), 676–681.

Smith, S., 2001. Chapter 5 Water resources, in: Wood, C.J.B. (Ed.), British Columbia, the Pacific Province: Geographical Essays, Department of Geography, University of Victoria, pp. 27-44.

Takeuchi, K., Hapuarachchi, P., Zhou, M., Ishidaira, H., Magome, J., 2008. A BTOP model to extend TOPMODEL for distributed hydrological simulation of large basins. Hydrological Processes 22, 3236–3251.

Tuller, S., 2001. Chapter 4 Climate, in: Wood, C.J.B. (Ed.), British Columbia, the Pacific Province: Geographical Essays, Department of Geography, University of Victoria, pp. 45-64.

US Army Corps of Engineers, 1980. Hydrographs by Single Linear Reservoir Model. Institute for Water Resources, Hydrologic Engineering Centre, TP-74, www.hec.usace.army.mil, (last access: July 14, 2015).

US Army Corps of Engineers, 1993. Introduction and Application of Kinematic Wave Routing Techniques Using HEC-1, TD-10. Institute for Water Resources, Hydrologic Engineering Centre, www.hec.usace.army.mil, (last access: November 31, 2015).

US Army Corps of Engineers, 2000. Hydrologic Modeling System HEC-HMS, Technical Reference Manual, March 2000, CPD-74B. Institute for Water Resources, Hydrologic Engineering Centre, www.hec.usace.army.mil, (last access: November 31, 2015).

Wikipedia, 2015. List of highest mountain peaks of Canada, https://en.wikipedia.org/wiki/List_of_highest_mountain_peaks_of_Canada, (last access: July 20, 2015).

Williams, J.R.; Hann, R.W., 1972. HYMO, a problem-oriented computer language for building hydrologic models, Water Resources Research, 8(1), 79-86.

Williams, J.R.; Hann, R.W., 1973. HYMO: Problem Oriented Computer Language for Hydrologic Modeling. USDA ARS-S-9. Washington, DC.

Wood, C.J.B., 2001. Chapter 1 Introduction, in: Wood, C.J.B. (Ed.), British Columbia, the Pacific Province: Geographical Essays, Department of Geography, University of Victoria, pp. 27-44.